ACS APPLIED MATERIALS & INTERFACES

Research Article

www.acsami.org

Analyzing Carbohydrate–Protein Interaction Based on Single Plasmonic Nanoparticle by Conventional Dark Field Microscopy

Hong-Ying Jin, Da-Wei Li,* Na Zhang, Zhen Gu, and Yi-Tao Long*

Key Laboratory for Advanced Materials & Department of Chemistry, East China University of Science and Technology, 130 Meilong Road, Shanghai 200237, People's Republic of China

Supporting Information

ABSTRACT: We demonstrated a practical method to analyze carbohydrate–protein interaction based on single plasmonic nanoparticles by conventional dark field microscopy (DFM). Protein concanavalin A (ConA) was modified on large sized gold nanoparticles (AuNPs), and dextran was conjugated on small sized AuNPs. As the interaction between ConA and dextran resulted in two kinds of gold nanoparticles coupled together, which caused coupling of plasmonic oscillations, apparent color changes (from green to yellow) of the single AuNPs were observed through DFM. Then, the color information was instantly transformed into a statistic peak wavelength distribution in less than 1 min by a self-developed statistical program (nanoparticleAnalysis). In addition, the interaction between ConA and dextran was proved with biospecific recognition. This approach is high-throughput and real-time, and is a convenient method to analyze carbohydrate–protein interaction at the single nanoparticle level efficiently.

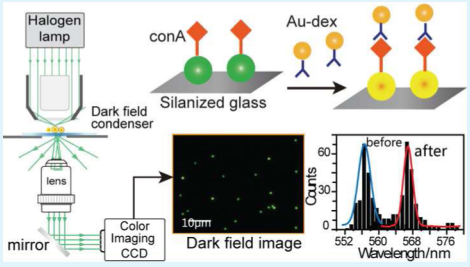

KEYWORDS: *carbohydrate–protein interaction, single plasmonic nanoparticle, dark field microscopy*

INTRODUCTION

Carbohydrate–protein interaction is correlated with multifarious biological processes, such as cell differentiation, virus infections, and cancer metastasis.[1−3] Many effectors affect the occurrence of specific carbohydrate–protein interaction and its strength to trigger relevant events. However, compared to antigen–antibody interactions, carbohydrate–protein interactions are typically low affinity, which makes relative studies more difficult.[4,5] The development of a new method to analyze carbohydrate–protein interactions will raise a better understanding of pathophysiological and physiological processes in living organisms, which is essential for the development of clinical diagnostics and therapeutic methods.

Gold nanoparticles (AuNPs) are used mostly for characterizing lectin–carbohydrate interactions due to their inherent properties such as the accessibility of preparation with well-defined shapes and sizes, robustness, easy surface modification, and good biocompatibility.[6−11] In addition, AuNPs exhibit excellent optical properties such as strong optical absorption, scattering due to localized surface plasmon resonance (LSPR) which are influenced by local dielectric environment,[12] as well as nanoparticles' shape and size.[13−15] Generally, methods for characterizing carbohydrate–protein interaction are involved in such a plasmonic property of AuNPs;[16−20] however, most of the traditional approaches are based on the averaged signals taken from multiple nanoparticles. Notably, each single nanoparticle could function as an independent detection sensor to provide significant signals with excellent signal-to-noise ratio.[21−23] Studies on the carbohydrate–protein interaction based on single nanoparticles are very rare, and could only detect the signal from several particles by special apparatus with high cost and complex systems. For example, an inverted fluorescent microscope and an electron-multiplied charge coupled device were used to study carbohydrate–protein interaction on single AuNPs,[24] which is novel but also quite expensive and complicated.

Herein, we developed a very simple and less costly method for the real-time and high-throughput analysis of the carbohydrate–protein interaction instantly. This approach was carried out with a conventional dark field microscopy (DFM) instrument with an imaging CCD at the single nanoparticle level, and the data was finally analyzed by a self-developed statistical program (nanoparticleAnalysis). DFM is highly sensitive and direct to probe chemical analytes.[25−27] However, the application of DFM to analyze chemical reactions is rare,[28] especially for the analysis of low affinity interactions. As several plasmonic nanoparticles were in close proximity to each other, a notable spectral red shift and obvious color changes in DFM were observed due to their plasmonic oscillations coupled together.[29−32] When one AuNP was modified with carbohydrate and another AuNP was conjugated with protein, the interaction between protein and carbohydrate could induce the two AuNPs coupled together, thus resulting in a color change of AuNPs observed by DFM. Then the color information on hundreds of nanoparticles in the DFM image was instantly transformed into a wavelength shift within 1 min by the nanoparticleAnalysis program.[33,34] The protein used in the experiment was concanavalin A (ConA), a carbohydrate

Received: March 30, 2015
Accepted: May 19, 2015
Published: May 19, 2015

DOI: 10.1021/acsami.5b02744
ACS Appl. Mater. Interfaces 2015, 7, 12249−12253

binding protein isolated from *Canavalia ensiformis* (jack bean), and the carbohydrate was dextran, a glucose polymer. Figure 1

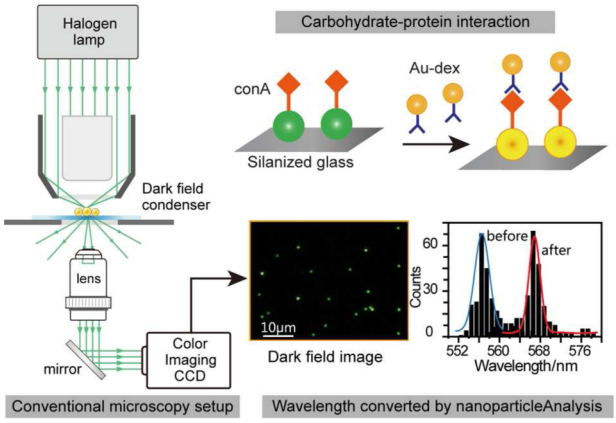

Figure 1. Schematic of carbohydrate−protein interaction analysis system by conventional dark field microscopy based on single gold nanoparticle. The left part is the setup of dark field microscopy equipped with an imaging CCD; the upper right corner is the schematic diagram of our experiment; the lower right part is the signal transform pattern.

shows the dark field microscope setup and our experimental process. To the best of our knowledge, this is the first example that a carbohydrate−protein interaction has been analyzed according to the color change in DFM at the single nanoparticle level, which is a valuable and low-cost technique for real-time detection of low affinity interactions.

EXPERIMENTAL SECTION

Preparation of Dextran-Capped AuNPs. Dextran was used as both a reducing agent and a stabilizer to prepare dextran-capped AuNPs (Au−dex) in one pot as described previously.[35] Briefly, 47.0 mL of Milli-Q purified water, 2.0 mL of 1.0% (w/w) $HAuCl_4$, and 20.0 mg of dextran were mixed in a clean beaker with ultrasonic irradiation for 20 min. Then, the pH of the solution was rapidly adjusted to 11 by quickly adding 1.0 mL of 1.0 mol/L NaOH under vigorous magnetic stirring, and the color of the solution changed to deep red within 30 min. The solution was washed three times through centrifugation (9000 rpm for 8 min) and resuspended in 10 mM sodium phosphate buffer solution (PBS) containing 0.1 mM Ca^{2+} and 0.1 mM Mn^{2+}. The concentration of prepared Au−dex was about 4.5×10^{-8} M, then the dextran−capped AuNPs solution was stored at 4 °C for use.

Preparation of 60 nm AuNPs. The preparation of AuNPs seed with diameters of 13 nm complied with a procedure that has been described previously.[36] Briefly, a 100 mL round-bottomed flask was equipped with a condenser, then 50 mL of 0.01 wt % $HAuCl_4$ was added. The solution was heated under vigorous stirring until boiling. Then 5 mL of 38.8 mM sodium citrate, which functioned as a reducing agent, was rapidly added to the solution. The color of the solution changed from yellow to red, which indicated the formation of seed AuNPs. The solution was stirred for an additional 15 min in air after heat treatment for 15 min.

The 60 nm gold nanoparticles were prepared from the seed nanoparticles as described previously.[37] Briefly, 1 mL of seed nanoparticles solution, 25 mL water, and 100 μL of 0.2 M NH_2OH·HCl solution were mixed in a 50 mL beaker. Then 3.0 mL of 0.1 wt % $HAuCl_4$ was added under vigorous stirring. With the dropwise addition of the $HAuCl_4$ solution, the color of the mixture gradually changed to brick-red. When the UV−vis wavelength was about 534 nm, it indicated that the gold nanoparticles diameter had come to 60 nm, and the addition of $HAuCl_4$ solution could be stopped. At last, the nanoparticle solution about 2.5×10^{-10} M was stored in a dark beaker at 4 °C.

Preparation of Samples. ConA modified gold nanoparticles were immobilized on a silanized glass slide. To perform scanning electron microscopy (SEM) experiments, the indium tin oxide (ITO) slide was selected due to its electroconductivity. First, the surfaces of ITO slides were cleaned by the piranha solution. ***Caution***: *piranha solution is aggressive and explosive. Never mix piranha waste with solvents. Check the safety precautions before using it.* The ITO slides (20 mm × 10 mm × 1.1 mm) were immersed in 20 mL of piranha solution and heated at 80 °C for 1h. Then, ultrapure water and ethanol were successively used to wash the ITO slides by ultrasonic irradiation for several times. The clean ITO slides were silanized by incubating them in ethanol solution containing 6% (v/v) Triethoxyoctylsilane for 4 h and were then rinsed with ethanol several times before dried at 110 °C for 1 h. The silanized ITO slides were then modified with AuNPs via adsorption by means of placing them in a 1.25×10^{-10} M gold colloid (60 nm) solution for 4 min. The AuNP functionalized ITO slides were rinsed with deionized water and dried under a stream of nitrogen prior to the addition of 0.1 μM ConA solution in 10 mM buffer solution (PBS, pH = 7.4) containing 0.1 mM Ca^{2+} and 0.1 mM Mn^{2+}. After 2 h, ConA was modified on the AuNPs through physical adsorption. The Au−ConA functionalized ITO slides were similarly rinsed with PBS (pH = 7.4) and dried under a stream of nitrogen before observed under the dark field microscope.

UV−vis Analysis of Carbohydrate−Protein Interaction. First, the prepared Au−dex 200 μL was diluted with PBS solution for 1.5 times, and then ConA was added in with final concentrations of 4, 7, 10, 13, and 16 nM, respectively. Then, The UV−vis spectra were acquired after 20 min.

Single Nanoparticle Measurement with Dark Field Microscopy. The dark field measurements were performed on an inverted microscope (eclipse Ti−U, Nikon, Japan) that was equipped with a 40× objective lens (NA = 0.8) and a dark field condenser (0.8 < NA < 0.95). The AuNPs slides were immobilized on a platform, and a 100 W halogen lamp providing a white light source was used to excite the AuNPs and to produce plasmon resonance scattering light. The dark field color images were acquired by a true-color digital camera (Nikon DS-fi, Japan). At first, the dark field color image of the Au−ConA nanoparticles was captured in the buffer solution. Then, the Au−dex solution was added to the slides with a concentration of 1.5×10^{-9} M. After reaction for 20 min, the water drop on the slide was removed and replaced by the buffer solution, and a dark field image of single nanoparticles was obtained to analyze carbohydrate−protein interaction.

RESULTS AND DISCUSSION

UV−vis Analysis of the Interaction between ConA and Au−dex. First, we analyzed aggregation of the nanoparticles due to the addition of ConA by UV−vis spectrometry. At pH 7.4 and room temperature, ConA is primarily present as a tetramer with four binding sites and one per subunit.[38] Therefore, the binding of ConA molecules to Au−dex nanoparticles resulted in cross-linking of several nanoparticles. When ConA was added to the Au−dex solution, there was an obvious red shift in the UV−vis spectrum, and 20 min later, there was no longer a peak shift observed (see the Supporting Information, Figure S5), which indicated that the interaction between ConA and dextran could be finished within 20 min. ConA with concentrations ranging from 0 to 16 nM could lead to the UV−vis peak wavelength shifted from 521 to 543 nm. The red shift was increased apparently and a broadening of the absorption spectrum was also observed with increasing concentrations of ConA, as shown in Figure 2. This was because with addition of ConA to the Au−dex solution, multiple binding events occur between ConA and the dextran immobilized on the particle surface, leading to cross-linking of

DOI: 10.1021/acsami.5b02744
ACS Appl. Mater. Interfaces 2015, 7, 12249−12253

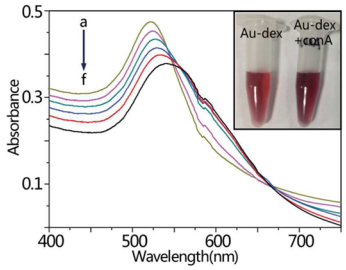

Figure 2. UV−vis spectra of Au−dex with different concentrations of ConA: 0 nM (a), 4 nM (b), 7 nM (c), 10 nM (d), 13 nM (e), and 16 nM (f); the inset figure illustrates the color change observed by naked eye before and after the addition of ConA.

the AuNPs. In addition, there was a clear color change of the Au−dex solution when 16 nM ConA was added in (see the inset picture in Figure 2). The color of the Au−dex solution was red, and it obviously changed to dark-red in 20 min due to Au−dex nanoparticles aggregated by ConA. Then we chose 20 min as the reaction time to do the following experiment.

Detection of Interaction between Au−ConA Nanoparticles and Au−dex at Single Nanoparticle Level. To characterize the interaction between ConA and Au−dex at the single nanoparticle level, we immobilized 60 nm gold nanoparticles on a silanized ITO slide, and then modified the gold nanoparticles with ConA by direct adsorption (for the procedure, see the Experiment Section). Adsorption time of AuNPs to the slide was 4 min, and after modified with ConA, the concention of Au−dex added to the slide was 1.5×10^{-9} M found to be the optimum condition (see the Supporting Information, Figures S6−S8). The scattering green spots in the captured DFM image corresponded to the individual nanoparticles modified with ConA (Au−ConA), as shown in Figure 3a.

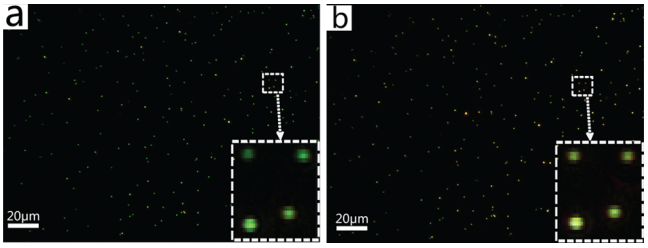

Figure 3. Dark field image of Au−ConA nanoparticles (a) and Au−ConA interacted with Au−dex nanoparticles (b).

When Au−dex nanoparticles were added to the slide, the color of the green scattering spots in the DFM images gradually turned yellow in 20 min, as shown in Figure 3b. The extent of color change was not identical for different individual nanoparticles. The binding ability and the number of ConA absorbed on the gold nanoparticle could explain the difference. This result indicated that ConA interacted with Au−dex, thus resulting in an obvious color change observed in the DFM images due to the two gold nanoparticles' plasmonic oscillations coupled together. To give exact proof that the color change of these nanoparticles in DFM image resulted from the coupling of the two particles, SEM images of assembled nanoparticles after the carbohydrate−protein interaction were taken, as shown in Figure 4. From the SEM images, it was clear to see that each large sized gold

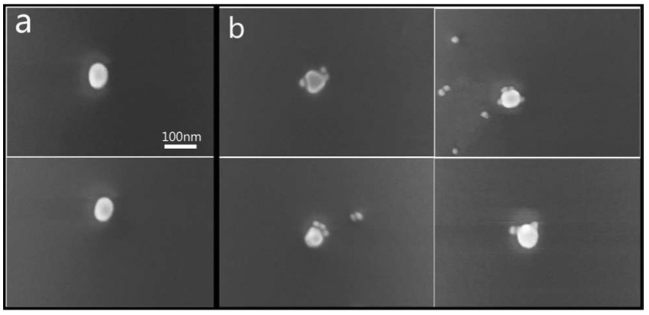

Figure 4. SEM images of Au−ConA nanoparticles (a) and Au−ConA interacted with Au−dex nanoparticles (b).

nanoparticle bound with three or four small sized gold nanoparticles, which is related to the color of single nanoparticle in DFM image, indicating that interaction between ConA and dextran resulted in the coupling of the two particles. The signals acquired from single nanoparticles revealed the information on every individual nanoparticle, which provide visualized results that help us a better understanding of carbohydrate−protein interaction.

Dark Field Analysis of Interaction between ConA and Dextran Statistically. As the DFM images of Au−ConA nanoparticles were captured before and after interaction with Au−dex, the scattering peak wavelength (λ_{max}) distribution of these single nanoparticles was calculated from the RGB (red, green, and blue) information in DFM color images by the nanoparticleAnalysis program, as shown in Figure 5a,b.

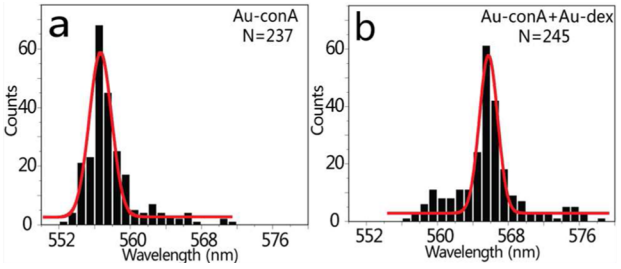

Figure 5. Statistic peak wavelength distribution calculated by nanoparticleAnalysis program: Au−ConA (a) and Au−ConA + Au−dex (b).

In color images, each pixel has 24 bits, including three 8-bit integers (0−255) that indicate the RGB colors' intensity. First, each color is deconstructed into RGB values that reflect information on the chromaticity and intensity, then the chromaticity values are transferred into a spectral wavelength of the scattering light. The spectral wavelength with the maximum intensity is known as the peak wavelength. The nanoparticleAnalysis program was used to acquire the peak wavelength distribution in DFM image within less than 1 min.[33,34] The red line is the Gaussian fitting for the histogram, we could see that the calculated peak wavelength of Au−ConA nanoparticles was at 556.7 nm before interaction (a) and it shifted to 565.8 nm after interaction with Au−dex (b). There is about a 9.1 nm red shift resulted from the carbohydrate−protein interaction, which caused coupling of the two gold nanoparticle. The statistic data showed overall change of numerous nanoparticles and corresponded to the change of single nanoparticles, which demonstrated that the statistic data and the single nanoparticles' signal could support each other.

DOI: 10.1021/acsami.5b02744
ACS Appl. Mater. Interfaces 2015, 7, 12249−12253

The convergent statistic data also manifested that this method is reliable and highly reproducible

Selective Detection. We also investigated the selectivity when Au−dex interacted with different proteins including carbohydrate−binding proteins like WGA (wheat germ agglutinin), PNA (peanut agglutinin), and SBA (soybean agglutinin), and noncarbohydrate−binding proteins such as PEP (pepsin) and BSA (bull serum albumin).

Color changes observed from dark field images and the peak wavelength distribution changes acquired from Gaussian fitting for the histogram of these gold nanoparticles after carbohydrate−protein interaction are shown in Figure 6. Table 1 lists

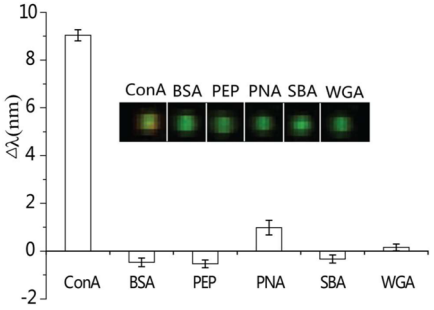

Figure 6. Changes of peak wavelength distribution acquired from Gaussian fitting of the histogram and dark field images of single gold nanoparticles (the inset picture) after carbohydrate−protein interaction in the presence of different proteins.

Table 1. Distribution of Peak Wavelength Given by Gaussian Fitting of Nanoparticle Scattering Peak Wavelength Histogram before and after Interaction with Different Proteins

protein	$\lambda_{wavelength}$ before interaction (nm)	$\lambda_{wavelength}$ after interaction (nm)	D-value (nm)
ConA	556.7 ± 0.30	565.8 ± 0.26	9.1 ± 0.40
BSA	557.5 ± 0.18	557.1 ± 0.15	−0.4 ± 0.23
PEP	558.9 ± 0.15	558.4 ± 0.13	−0.5 ± 0.20
PNA	559.0 ± 0.23	560.0 ± 0.20	1.0 ± 0.30
SBA	558.5 ± 0.14	558.2 ± 0.13	−0.3 ± 0.19
WGA	557.7 ± 0.11	557.9 ± 0.14	0.2 ± 0.18

the calculated peak wavelengths for different Au−protein nanoparticles before and after interaction with Au−dex nanoparticles. Remarkably, when ConA was substituted by these proteins, no matter the carbohydrate-binding proteins or noncarbohydrate-binding proteins, neither the color changes in the DFM image nor an apparent peak shift of the calculated peak wavelength distribution was observed at the same concentration of Au−dex (for the DFM images and the Gaussian fitting of the statistic peak wavelength histogram, see the Supporting Information, Figures S9−S18). Only the presence of ConA could induce the coupling of the gold nanoparticles, which affirmed that the coupling was mediated by the interaction of ConA and dextran. These results further confirmed that the interaction between ConA and dextran occurred by means of biospecific molecular recognition. Compared to sensing chemical reaction, a strong interaction such as click reaction based on the scattering properties of gold nanoparticles,[39] the proposed high-throughput method could be used to analyze the low binding affinity of carbohydrate−protein interaction in real-time via conventional dark field microscopy.

CONCLUSION

In conclusion, we developed an available and quite rapid method for real-time analysis of the carbohydrate−protein interaction with the example of ConA and dextran at the single nanoparticle level by DFM. When large sized AuNPs modified with ConA, small sized AuNPs conjugated with dextran, carbohydrate−protein interaction on the surface of single gold nanoparticles could lead to interparticle coupling, which resulted in color changes in the DFM image. Not only could we get the single nanoparticles' signal but also we could acquire statistic information on the scattering peak wavelength calculated by nanoparticleAnalysis program. Our studies demonstrated the feasibility to use DFM to investigate the low affinity interaction between carbohydrate and protein at the single nanoparticle level, which lay a foundation for the application of practical sample related to carbohydrate−protein interaction.

ASSOCIATED CONTENT

Supporting Information

UV−vis measurement of Au−dex and Au (60 nm) (Figures S1, S2), TEM characterization of Au−dex and Au (60 nm) (Figures S3, S4), time-dependent UV−vis analysis of the interaction between ConA and dextran (Figure S5), dark field experiment conditions (Figures S6−S8), dark field images and statistic wavelength distribution of single gold nanoparticles modified with proteins (BSA, PEP, PNA, SBA, WGA) before and after interaction with Au−dex (Figures S9−S18). The Supporting Information is available free of charge on the ACS Publications website at DOI: 10.1021/acsami.5b02744.

AUTHOR INFORMATION

Corresponding Authors

*Y.-T. Long. E-mail: ytlong@ecust.edu.cn.
*D.-W. Li. E-mail: ldwiqj@gmail.com.

Notes

The authors declare no competing financial interest.

ACKNOWLEDGMENTS

This work was supported by the National Science Fund of China (21421004 and 21327807) and National Base Research 973 Program (2013CB733700). Y.-T. Long is supported by the National Science Fund for Distinguished Young Scholars of China (21125522).

REFERENCES

(1) Robinson, M. J.; Sancho, D.; Slack, E. C.; LeibundGut-Landmann, S.; Sousa, C. R. e. Myeloid C-type Lectins in Innate Immunity. *Nat. Immunol.* **2006**, *7*, 1258−1265.
(2) Bertozzi, C. R.; Kiessling, L. L. Chemical Glycobiology. *Science* **2001**, *291*, 2357−2364.
(3) Lever, R.; Page, C. R. Novel Drug Development Opportunities for Heparin. *Nat. Rev. Drug. Discovery* **2002**, *1*, 140−148.
(4) Lee, Y. C.; Lee, R. T. Carbohydrate-Protein Interactions: Basis of Glycobiology. *Acc. Chem. Res.* **1995**, *28*, 321−327.
(5) Weis, W. I.; Drickamer, K. Structural Basis of Lectin-Carbohydrate Recognition. *Annu. Rev. Biochem.* **1996**, *65*, 441−473.
(6) Daniel, M. C.; Astruc, D. Gold Nanoparticles: Assembly, Supramolecular Chemistry, Quantum-Size-Related Properties, and

DOI: 10.1021/acsami.5b02744
ACS Appl. Mater. Interfaces 2015, 7, 12249−12253

Applications toward Biology, Catalysis, and Nanotechnology. *Chem. Rev.* **2004**, *104*, 293−346.
(7) Anker, J. N.; Hall, W. P.; Lyandres, O.; Shah, N. C.; Zhao, J.; Van Duyne, R. P. Biosensing with Plasmonic Nanosensors. *Nat. Mater.* **2008**, *7*, 442−453.
(8) Stewart, M. E.; Anderton, C. R.; Thompson, L. B.; Maria, J.; Gray, S. K.; Rogers, J. A.; Nuzzo, R. G. Nanostructured Plasmonic Sensors. *Chem. Rev.* **2008**, *108*, 494−521.
(9) Jain, P. K.; Huang, X.; El-Sayed, I. H.; El-Sayed, M. A. Noble Metals on the Nanoscale: Optical and Photothermal Properties and Some Applications in Imaging, Sensing, Biology, and Medicine. *Acc. Chem. Res.* **2008**, *41*, 1578−1586.
(10) Sperling, R. A.; Gil, P. R.; Zhang, F.; Zanella, M.; Parak, W. J. Biological Applications of Gold Nanoparticles. *Chem. Soc. Rev.* **2008**, *37*, 1896−1908.
(11) Sardar, R.; Funston, A. M.; Mulvaney, P.; Murray, R. W. Gold Nanoparticles: Past, Present, and Future. *Langmuir* **2009**, *25*, 13840−13851.
(12) Ghosh, S. K.; Nath, S.; Kundu, S.; Esumi, K.; Pal, T. Solvent and Ligand Effects on the Localized Surface Plasmon Resonance (LSPR) of Gold Colloids. *J. Phys. Chem. B* **2004**, *108*, 13963−13971.
(13) Maye, M. M.; Han, L.; Kariuki, N. N.; Ly, N. K.; Chan, W. B.; Luo, J.; Zhong, C. Gold and Alloy Nanoparticles in Solution and Thin Film Assembly: Spectrophotometric Determination of Molar Absorptivity. *Anal. Chim. Acta* **2003**, *496*, 17−27.
(14) Liu, X.; Atwater, M.; Wang, J.; Huo, Q. Extinction Coefficient of Gold Nanoparticles with Different Sizes and Different Capping Ligands. *Colloid Surf., B* **2007**, *58*, 3−7.
(15) Wiley, B. J.; Im, S. H.; Li, Z. Y.; McLellan, J.; Siekkinen, A.; Xia, Y. Maneuvering the Surface Plasmon Resonance of Silver Nanostructures through Shape-Controlled Synthesis. *J. Phys. Chem. B* **2006**, *110*, 15666−15675.
(16) Lee, S.; Pérez-Luna, V. H. Dextran-Gold Nanoparticle Hybrid Material for Biomolecule Immobilization and Detection. *Anal. Chem.* **2005**, *77*, 7204−7211.
(17) Mislovičová, D.; Masarova, J.; Švitel, J.; Gemeiner, P. Influence of Mannan Epitopes in Glycoproteins−Concanavalin A Interaction. Comparison of Natural and Synthetic Glycosylated Proteins. *Int. J. Biol. Macromol.* **2002**, *30*, 251−258.
(18) Bellapadrona, G.; Tesler, A. B.; Grünstein, D.; Laila, H. H.; Raghavendra, K.; Peter, H. S.; Alexander, V.; Israel, R. Optimization of Localized Surface Plasmon Resonance Transducers for Studying Carbohydrate−Protein Interactions. *Anal. Chem.* **2011**, *84*, 232−240.
(19) Otten, L.; Richards, S. J.; Fullam, E.; Gurdyal, S. B.; Matthew, I. G. Gold Nanoparticle-Linked Analysis of Carbohydrate−Protein Interactions, and Polymeric Inhibitors, Using Unlabelled Proteins; Easy Measurements Using a 'Simple' Digital Camera. *J. Mater. Chem. B* **2013**, *1*, 2665−2672.
(20) Tsai, C. S.; Yu, T. B.; Chen, C. T. Gold Nanoparticle-based Competitive Colorimetric Assay for Detection of Protein−Protein Interactions. *Chem. Commun.* **2005**, *34*, 4273−4275.
(21) McFarland, A. D.; Van Duyne, R. P. Single Silver Nanoparticles as Real-Time Optical Sensors with Zeptomole Sensitivity. *Nano Lett.* **2003**, *3*, 1057−1062.
(22) Berciaud, S.; Cognet, L.; Tamarat, P.; Lounis, B. Observation of Intrinsic Size Effects in the Optical Response of Individual Gold Nanoparticles. *Nano Lett.* **2005**, *5*, 515−518.
(23) Cao, C.; Sim, S. J. Resonant Rayleigh Light Scattering Response of Individual Au Nanoparticles to Antigen−Antibody Interaction. *Lab Chip* **2009**, *9*, 1836−1839.
(24) Liu, X.; Zhang, Q.; Tu, Y.; Zhao, W. F.; Gai, H. W. Single Gold Nanoparticle Localized Surface Plasmon Resonance Spectral Imaging for Quantifying Binding Constant of Carbohydrate−Protein Interaction. *Anal. Chem.* **2013**, *85*, 11851−11857.
(25) Qu, W. G.; Deng, B.; Zhong, S. L.; Shi, H. Y.; Wang, S. S.; Xu, A. W. Plasmonic Resonance Energy Transfer-based Nanospectroscopy for Sensitive and Selective Detection of 2,4,6-Trinitrotoluene (TNT). *Chem. Commun.* **2011**, *47*, 1237−1239.
(26) Raschke, G.; Kowarik, S.; Franzl, T.; Sçnnichsen, C.; Klar, T. A.; Feldmann, J.; Nichtl, A.; Krzinger, K. Biomolecular Recognition Based on Single Gold Nanoparticle Light Scattering. *Nano Lett.* **2003**, *3*, 935−938.
(27) Yguerabide, J.; Yguerabide, E. E. Light-Scattering Submicroscopic Particles as Highly Fluorescent Analogs and Their Use as Tracer Labels in Clinical and Biological Applications: I. Theory. *Anal. Biochem.* **1998**, *262*, 137−156.
(28) Novo, C.; Funston, A. M.; Mulvaney, P. Direct Observation of Chemical Reactions on Single Gold Nanocrystals Using Surface Plasmon Spectroscopy. *Nat. Nanotechnol.* **2008**, *3*, 598−602.
(29) Chen, J. I. L.; Chen, Y.; Ginger, D. S. Plasmonic Nanoparticle Dimers for Optical Sensing of DNA in Complex Media. *J. Am. Chem. Soc.* **2010**, *132*, 9600−9601.
(30) Chen, J. I. L.; Durkee, H.; Traxler, B.; Ginger, D. S. Optical Detection of Protein in Complex Media with Plasmonic Nanoparticle Dimers. *Small* **2011**, *7*, 1993−1997.
(31) Guo, L. H.; Ferhan, A. R.; Chen, H.; Li, C. M.; Chen, G. N.; Hong, S.; Kim, D. H. Distance-Mediated Plasmonic Dimers for Reusable Colorimetric Switches: A Measurable Peak Shift of More than 60 nm. *Small* **2013**, *9*, 234−240.
(32) Liu, N.; Hentschel, M.; Weiss, T.; Alivisatos, A. P.; Giessen, H. Three-Dimensional Plasmon Rulers. *Science* **2011**, *332*, 1407−1410.
(33) Jing, C.; Gu, Z.; Ying, Y. L.; Li, D. W.; Zhang, L.; Long, Y. T. Chrominance to Dimension: A Real-Time Method for Measuring the Size of Single Gold Nanoparticles. *Anal. Chem.* **2012**, *84*, 4284−4291.
(34) Gu, Z.; Jing, C.; Ying, Y. L.; He, P. G.; Long, Y. T. In Situ High Throughput Scattering Light Analysis of Single Plasmonic Nanoparticles in Living Cells. *Theranostics* **2015**, *5*, 188−195.
(35) Nath, S.; Kaittanis, C.; Tinkham, A.; Perez, J. M. Dextran-Coated Gold Nanoparticles for the Assessment of Antimicrobial Susceptibility. *Anal. Chem.* **2008**, *80*, 1033−1038.
(36) Grabar, K. C.; Freeman, R. G.; Hommer, M. B.; Natan, M. J. Preparation and Characterization of Au Colloid Monolayers. *Anal. Chem.* **1995**, *67*, 735−743.
(37) Link, S.; El-Sayed, M. A. Size and Temperature Dependence of the Plasmon Absorption of Colloidal Gold Nanoparticles. *J. Phys. Chem. B* **1999**, *103*, 4212−4217.
(38) Huet, M. Factors Affecting the Molecular Structure and the Agglutinating Ability of Concanavalin A and Other Lectins. *Eur. J. Biochem.* **1975**, *59*, 627−632.
(39) Shi, L.; Jing, C.; Ma, W.; Li, D. W.; Jonathan, E. H.; Frank, M.; Long, Y. T. Plasmon Resonance Scattering Spectroscopy at the Single-Nanoparticle Level: Real-Time Monitoring of a Click Reaction. *Angew. Chem., Int. Ed.* **2013**, *52*, 6011−6014.

DOI: 10.1021/acsami.5b02744
ACS Appl. Mater. Interfaces 2015, 7, 12249−12253